Welding in the World (2022) 66:611–628
https://doi.org/10.1007/s40194-021-01229-6

REVIEW ARTICLE

# In situ detection of welding defects: a review

**Anirudh Sampath Madhvacharyula[1] · Araveeti V Sai Pavan[2] · Subrahmanyam Gorthi[2] · Srihari Chitral[1] · N Venkaiah[1] · Degala Venkata Kiran[1]**

Received: 29 July 2021 / Accepted: 30 November 2021 / Published online: 21 January 2022


**Abstract**
Weld defect detection is a crucial aspect for improving the productivity and quality of the welding process. Several non-destructive methods exist for the identification of defects post weld deposition. However, they only help assess the quality of the component and offer no inputs while the welding process is being performed. Real-time or in situ weld defect detection aids in the detection of defects during the welding process, allowing to take corrective measures or halt the welding to avoid further wastage of time and material. The current paper provides a brief description of various types of weld defects and the commonly used non-destructive testing (NDT) techniques used for identifying weld defects. It then proceeds to provide a detailed review of various methods available for in situ weld defect detection, classifying them based on their input signals. It also classifies the methods based on the type of algorithm used, along with an intuitive explanation of the commonly used algorithms in weld defect detection. The methods covered in this manuscript make use of different input signals that include audio, welding current and voltage, and optical signals also highlighting methods that use a combination of the abovementioned signals for in situ prediction of weld defects. A critical analysis of the efficacy, advantages, and drawbacks of each method is presented. Further, this work highlights a few research gaps identifying avenues for future research in this area.

**Keywords** In situ weld defect detection · Welding current and voltage signals · Arc images · Spectroscopy · IR thermography · Acoustic emissions · Multi-sensor defect detection

## 1 Introduction

Welding plays a pivotal role in several industries including automobile, aerospace, oil, gas, and space exploration. Weld monitoring is an essential aspect of welding to ensure quality output and detect any defects that might be detrimental to the life of welded structure, leading to safety hazards. Weld monitoring also plays a vital role while designing feedback systems for robotic welding, where parameters have to be altered in real time to account for any aberrations from the desired mode of welding. Defect detection is particularly beneficial in multi-pass welding processes and metal additive manufacturing, where defects in the initial layers can be detrimental and affect the integrity of subsequent layers.

Before getting into the various defect detection methods, it is helpful to have an understanding of the various types of defects and their causes. This will not only provide knowledge behind defect generation but will also give better insights in understanding why different methods work. Figure 1 shows the commonly observed defects in welding which include porosity, slag inclusion, incomplete fusion and penetration, cracks, and undercut [1]. The specific reasons behind the formation of porosity vary with the type of welding used. One of the causes for porosity in laser welding is due to unstable keyhole phenomena [2]. Vulnerability to porosity during welding also depends on the material used. Aluminum being highly reactive is more prone to porosity. In gas metal arc welding (GMAW) of galvanized steels, the zinc vapor emitted during the welding process is a significant factor causing porosity [3].

In most cases, porosity or blowholes occur due to trapped gases or contaminants on the weld surface. They

Recommended for publication by Commission V - NDT and Quality Assurance of Welded Products.

✉ Degala Venkata Kiran

[1] Department of Mechanical Engineering, Indian Institute of Technology Tirupati, Tirupati, India

[2] Department of Electrical Engineering, Indian Institute of Technology Tirupati, Tirupati, India

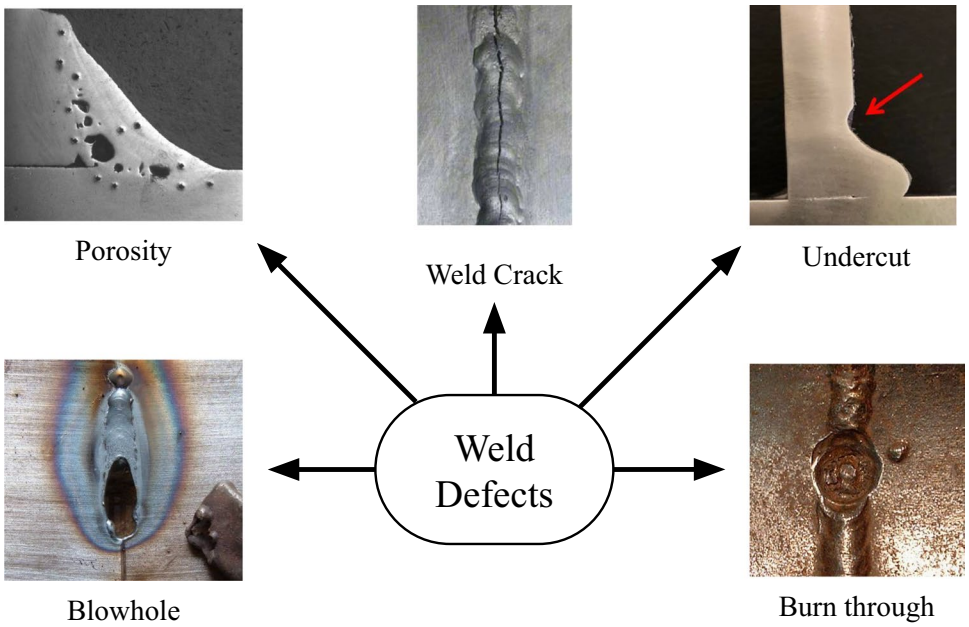


**Fig. 1** Commonly observed defects in real-time welding (the above images are taken from various sources for illustrative purpose)

can be minimized by ensuring proper welding current and deposition speed and thorough cleaning to prevent any contaminants from entering the weld zone. Slag inclusion, on the other hand, is caused by contaminants like oxides or fluorides getting trapped in the weld bead that can be prevented by proper cleaning of slag between subsequent layers and providing sufficient shielding gas during the welding process. Weld defects like incomplete fusion and lack of penetration can be reduced by optimizing the joint design, raising the temperature of the base metal and increasing the heat input during welding.

Cracks are one of the types of weld defects which can severely affect the life of a component. They are commonly caused by thermal stresses, uneven cooling rates, and embrittlement due to elements like sulfur or hydrogen. Hydrogen-induced cracking (HIC) is caused by the diffusion of hydrogen, leading to the embrittlement of joints. It depends on various factors such as the alloying elements used [4], hydrogen content [5], and residual stresses [6]. These defects can be avoided by using a proper joint design, using suitable weld parameters, preheating the components, and avoiding rapid cooling of the weld bead.

Defects in the weld profile like undercutting occur due to the melting of base metal which results in the formation of a notch that might act as a stress raiser and cause premature failure of the weld. Excessive heat input during welding can result in burn through, which is caused due to the collapse of the molten pool due to excessive penetration leaving a hole or cavity in the weld bead.

Weld defects are identified and characterized by subjecting the welded components to non-destructive testing methods. Figure 2 depicts the existing methods for NDT

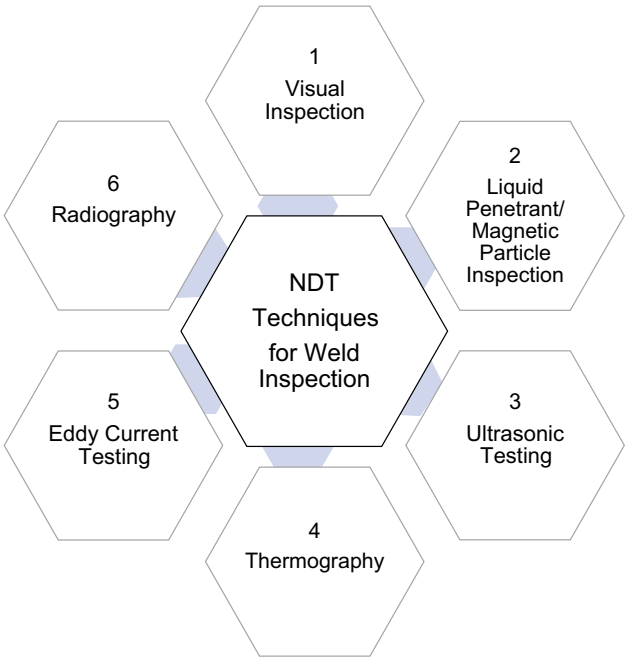


**Fig. 2** Overview of existing techniques for NDT of weld components

of weld joints. Rudimentary methods like visual inspection involve surveying the weld bead for any visible defects like undercuts, slag inclusion, blowholes, surface cracks, and porosity. These methods, however, require an experienced observer capable of identifying defects. In recent years, several algorithms have been developed to automate this process and improve the accuracy beyond human capabilities [7–9].

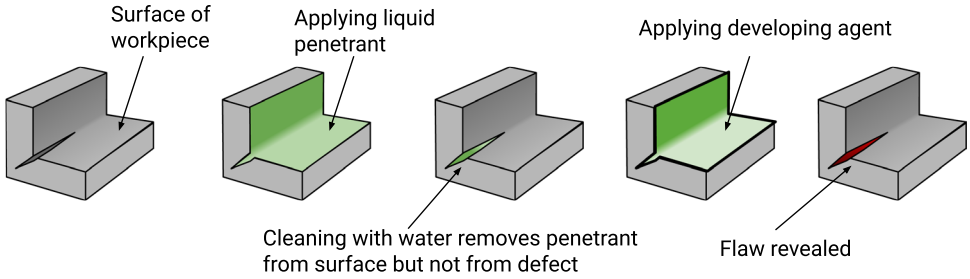


**Fig. 3** Liquid penetrant testing of manufactured components for identification of surface defects

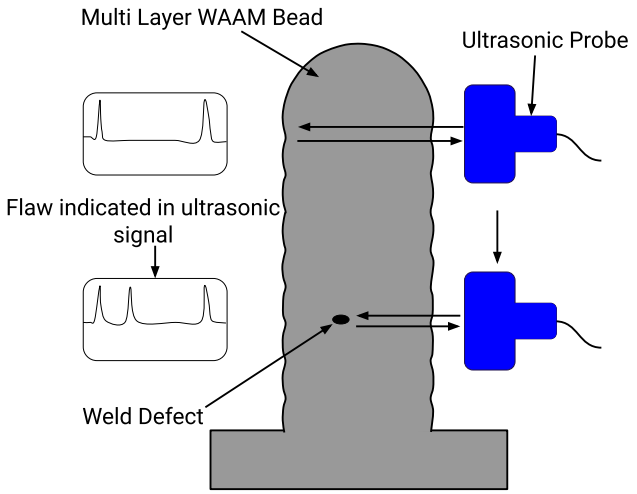


**Fig. 4** Schematic representation of ultrasonic testing for additively manufactured components

Visual inspection is often improved using liquid penetrants, usually visible or fluorescent penetrants, which highlight surface defects and making them easily identifiable as explained in Fig. 3. This method can detect surface defects as small as 0.1 $\mu$m. Magnetic particle inspection also works on a similar principle. However, this method uses magnetic particles spread out over the weld bead and a magnetic field to locate the defects [10]. All three methods mentioned above can detect only external defects like surface flaws that are open.

Other methods like ultrasonic testing (UT) are much more robust and are capable of defecting subsurface defects. The working principle of UT is depicted in Fig. 4. In this technique, ultrasonic beams are projected through the material; flaws in the beam's path partly reflect back the energy helping us locate and identify the defect. The ultrasonic signals reflected have been studied, and several analytical methods have been developed to analyze these signals to accurately identify the location and the type of the defects in both welded and additive manufactured components [11–15].

While UT is a contact method, non-contact methods like infrared (IR) thermography are also capable of detecting weld defects. IR thermography exploits the principle that defective weld regions absorb heat differently from areas with proper weld. The experimental setup for IR thermography is shown in Fig. 5. Several studies have been performed studying the uses of thermography for weld defect detection [16–20].

Another prominent non-contact method used to detect weld defects is eddy current testing (Fig. 6). The part is placed near or inside an alternating current coil; the current, by induction, causes eddy currents to flow inside the component. Defects in the part alter the flow of the eddy currents, affecting the exciting coil whose voltage is monitored closely to detect any imperfections [21–25].

Non-destructive techniques like radiography use X-ray images to detect internal flaws like cracks or porosity. The pores in welds usually appear in a darker shade in the radiographic images, as shown in Fig. 7. Radiographic images are often analyzed using computational techniques that can

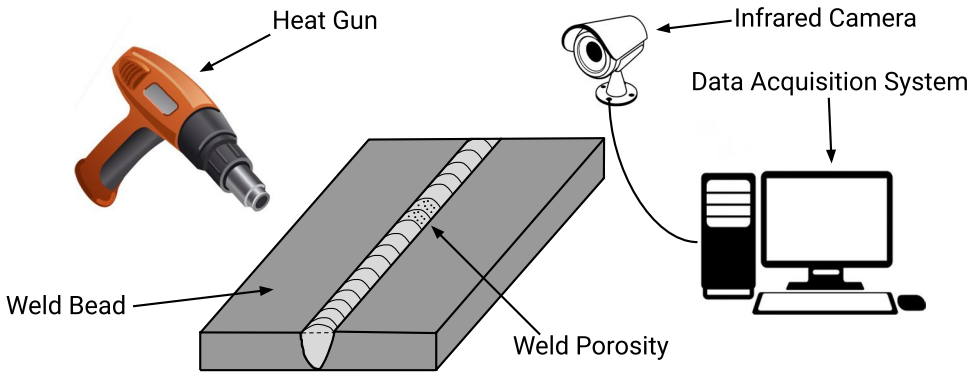


**Fig. 5** Experimental setup for weld defect detection using IR thermography

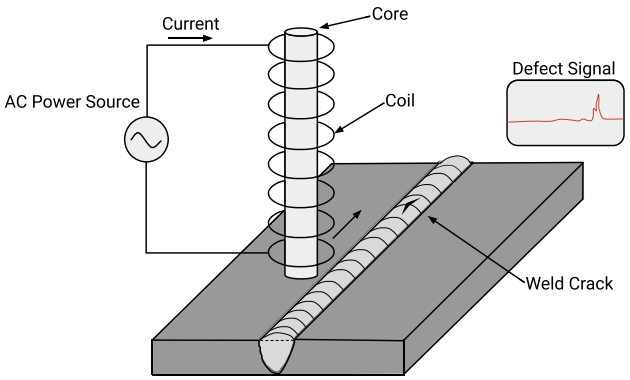


**Fig. 6** Analysis of defective weld bead using eddy current testing

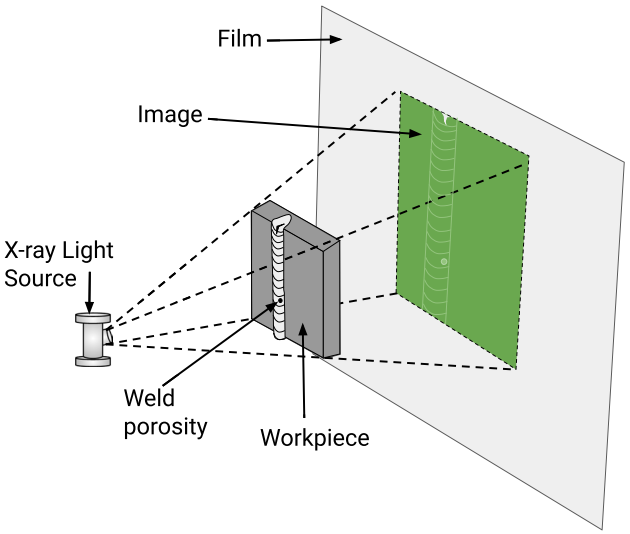


**Fig. 7** Schematic representation of experimental setup for recording radiographic images of weld bead

automatically detect and classify defective regions in a weld [26–29].

Non-destructive testing techniques are also used widely in multi-pass and metal additive manufacturing processes. Methods such as radiography and ultrasound can be extended to locate and characterize defects in additive manufactured components [30, 31]. With metal additive manufacturing being used extensively in large-scale manufacturing of complex components, adapting NDT techniques which are widely used in welding to evaluate the integrity of additive manufactured components is critical.

NDT methods are considerably effective in detecting defects accurately; however, these methods have a common drawback: all these techniques can detect defects only in the post-processing stage. Since the welding has already been completed by the time of defect detection, the component can only be discarded or recycled, both of which require additional time and energy. Moreover, material is wasted when the defective parts are discarded. Therefore, it is crucial that defects are detected in situ, i.e., during the process, to take necessary corrective measures to mitigate the adverse effects of the defect or halt the process and prevent further wastage of material. With today's technological advancements and having access to advanced sensors and greater computational power, it is possible to accurately collect and analyze data in minimal amounts of time, thus making in situ defect detection systems to be employed for real-time monitoring of welding. It is desirable that in situ methods have the capability to classify various types of flaws along with detecting them. The measures taken to prevent defects vary with the kind of defects.

This paper provides an overview of the existing methods of in situ defect detection in welding. Although several papers deal with detecting defects during welding, a thorough consolidation of in situ defect detection methods has not been reported yet. This paper presents a classification of these methods based on the type of acquired signal used to extract features for detecting defects and present the classification accuracy results. The following sections provide a detailed description of in situ weld defect detection techniques classified based on their input signals, viz., acoustic signals, optical sensors, welding current and voltage signals, and features obtained from multiple sensors as shown in Fig. 8. The later sections of the paper classify the algorithms used for weld defect detection, with an intuitive description of a few widely used algorithms. The current paper covers both conventional signal processing techniques and modern-day approaches like machine learning algorithms. Finally, a critical discussion on various methods, their advantages, and drawbacks is presented.

## 2 Defect detection using acoustic signals

The current section covers in situ weld defect detection using acoustic signals. It is classified into two classes, viz., audio signal- and acoustic signal-based defect detection. Audio signal-based defect detection analyzes audible sound signals emitted by the welding arc to identify weld defects. On the other hand, acoustic emission involves examining the acoustic waves emitted during the welding process to predict weld stability.

### 2.1 Audio signals

The use of audible sound signals provides a cost-effective method for in situ detection of weld defects. The notion of audio signals emitted being an indicator of weld defects was first studied by Saini et al. [32], in which statistical parameters of audio signals emitted for defective and non-defective

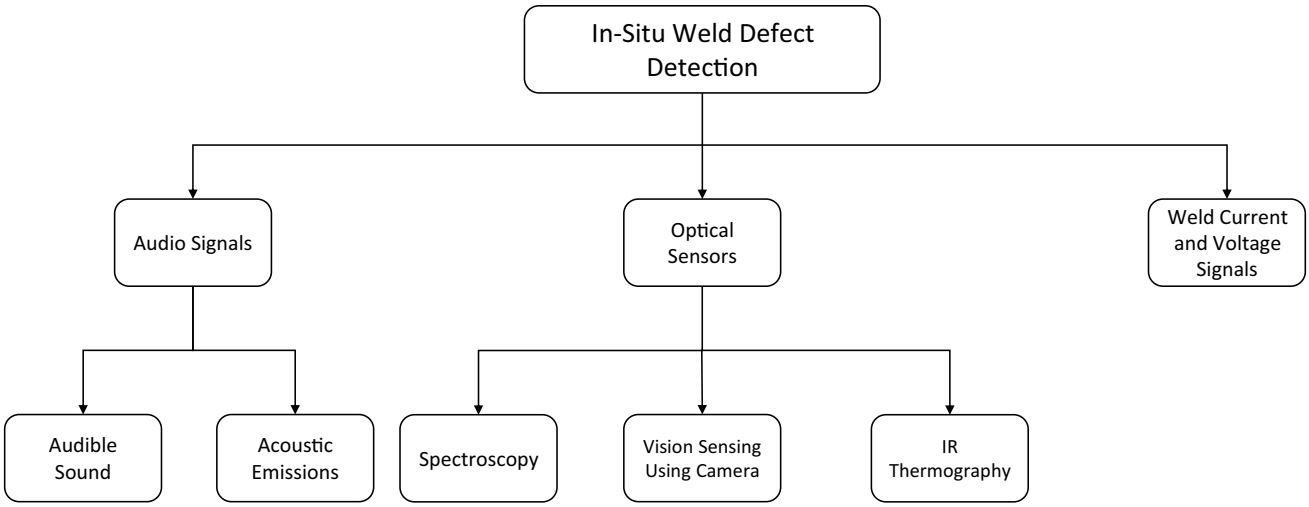


**Fig. 8** Signal based classification of in situ weld defect detection methods

welds were compared. The work concludes that parameters like zero crossing rate, root amplitude, and shape factor can aid weld defect detection, while others like impulse factor, peak factor, and clearance factor do not show much promise as they depend on the peak value of sound. The feasibility of sound signals for weld monitoring was also investigated by Grad et al. [33], highlighting that changes in parameters like kurtosis and power spectral density identified aberrations from usual arc behavior. Cudina et al. [34] studied the correlation between the arc sound and arc behavior. The paper established the connection between the arc behavior and the emitted audio signal, identifying arc extinction and re-ignition during short-circuiting as the major sources for generating sound.

The effect of metal transfer modes in pulsed gas metal arc welding (GMAW-P) process on arc sound was analyzed by Pal et al. [35, 36]. Their work found the root mean square (RMS) and kurtosis of sound signals to strongly correlate with pulse voltage parameters to help in identifying the metal transfer modes. Their findings also indicated that weld sound was a reliable indicator of defects. The use of sound signals for online monitoring has not been limited to GMAW alone but has also been pursued in laser welding and powder bed fusion processes. It is evident from the above studies that sound signals show promise for being used as inputs for weld defect detection algorithms.

Several investigations were conducted towards using the sound signal emitted to develop a system for online monitoring of welding. Yousof et al. [37] worked to develop a method for detecting porosity in weld pipeline steel. The research used empirical mode decomposition (EMD) and the Hilbert-Huang transform (HHT) to identify and locate weld defects. The audio signal emitted during the welding is first recorded using a piezoelectric microphone attached to the welding torch. The signal is then subjected to EMD, which decomposes the signal into several parts of narrower frequency bands. The resultant of the process of EMD is the intrinsic mode function (IMF). HHT is performed on the IMF signal to obtain the audio signal's power spectral density. The regions with surface and subsurface porosity are clearly highlighted in the plot of the Hilbert spectrum. The analysis, in short, provides insights into the weld pool oscillation behavior, enabling us to locate the defects.

Luo et al. [38] used wavelet analysis and ANNs to identify laser welding defects. The audio signal emitted is decomposed into several levels by using discrete wavelet analysis. This work involved performing level 5 decomposition of audio signals. Wavelet coefficients were given as input to a back-propagation neural network with a single hidden layer of 100 nodes. More intuitive explanation of wavelet transform is covered in a later section.

ANNs were also used by Pernambuco et al. [39] who proposed a non-intrusive methodology to identify the discontinuities during the metal inert gas (MIG)/metal active gas (MAG) welding process using the electric arc's sound signals. The method used a three-layer ANN to classify the discontinuities into three transfer modes. The proposed architecture consists of an input layer, three hidden layers, and an output layer. The trained binary classifiers for each transfer mode reported more than 90% accuracy and achieved a multi-class classification accuracy of 84%. Another time-frequency method to identify and locate weld defects was proposed by Sudhanya et al. [40]. The work studied the usefulness of the adaptive chirplet transform to detect welding defects. Chirplet transform [41] is similar to wavelet transform, the only difference being that a chirp is used to take the transform in place of a mother wavelet function. The occurrence of high chirps in the sound signal

correlated with weld defects. The use of audio signals is not limited to weld defect detection but also can be used to monitor other aspects like depth of weld [42]. Further, the properties of the weld bead can also be studied using this analysis technique.

Audible sound-based defect detection is therefore a cost-effective way to identify and locate defects. Audible sound is used to identify defects in a variety of industries like automobile and manufacturing. It can be a matter of interest to study the efficacy of algorithms found successful in other domains for weld defect detection. Another signal similar to audio signals is acoustic emissions which are covered in the following section.

### 2.2 Acoustic emissions

Acoustic emission (AE) testing is a method in which the acoustic waves released during a process are recorded using a sensor. The ultrasound stress waves emitted are captured by piezoelectric sensors and transformed to electrical signals which are further used for analysis. AE has been found useful for analyzing the stability of welds [43]. A statistical approach towards monitoring laser welding using acoustic emission signals was pursued by Gu et al. [44]. The AE signals recorded during real-time welding were compared to those of perfect welds made under optimal process conditions. The dominant frequencies in the AE signals vary with weld speed. The comparison of the two spectra was made by calculating the square of standard deviation of fast Fourier transform (FFT) component intensities in the 12–17 kHz region. Based on this, the weld was classified into full penetration, partial penetration, and overheated weld. This study indicated the feasibility of AE to be used for monitoring of laser welding.

Air coupled UT is a contact-free method which uses air as a medium for transmitting ultrasonic signals to characterize the material properties. Zhang et al. [45, 46] investigated the application of air coupled UT and AE in monitoring gas tungsten arc welding (GTAW) process. Their primary focus was on studying the burn through defect. Their AE signals provided insights into the welding quality, helping detect any localized discontinuities in the weld. An increase in the absolute energy of the AE signal is found to correspond to an increased supply of heat energy. The energy ratio of the UT signal and its peak frequency was indicative of the increase in weld penetration. The combination of UT and AE signals could give a detailed description of the welding processes.

The utility of AE signals emitted was also studied by Gaja et al. [47]. Several features of the AE signals were used to cluster the data and identify cracks or porosities in laser metal deposition. The AE signal features include peak amplitude, kurtosis, energy, and number of counts. Principal component analysis (PCA) was used for dimensionality reduction of the input features. The input features were clustered using K-means clustering [48]. The AE signal emitted in the presence of porosity had a shorter decay time and lower amplitude, while the signals with cracks had a short duration and high amplitudes. It has been found feasible to use AE signals with ANNs to model complex parameter relationships and evaluate the stability of the GMAW process [49]. Acoustic emissions have also been used for other forms of welding like friction stir welding [50]. Changming et al. [51] used the wavelet transform of AE to identify weld defect by observing changes in band energy.

Acoustic emissions are especially advantageous because of their fast response making them a favorable option for in situ weld monitoring and defect detection. However, it should also be kept in mind that these signals might be susceptible to external interference and therefore need necessary preprocessing steps to eradicate noise and amplify the signal. While audio signals involve the processing of 1-D signals to spot weld defects, methods using optical sensors involve capturing images (2-D signals) or spectral data for defect detection. The data is then analyzed using computer vision techniques or convolutional neural networks (CNNs) to identify weld defects.

## 3 Defect detection using optical sensors

The current section discusses in situ weld defect detection using optical sensors. It primarily deals with three main types of optical signals, viz., spectroscopy, vision sensing, and IR thermography which will be discussed individually in the same sequence.

### 3.1 Spectroscopy

Spectroscopic analysis of welding arc exploits the fact that different wavelengths of light are emitted by the weld arc during the welding process. The arc stability can be predicted based on the change in the intensities of different wavelengths emitted. The plasma spectrum captures emission lines at various wavelengths ranging from 100 to 900 nm emanated during the arc welding process. It was found that the estimated electronic temperature correlates with the weld quality. Several studies followed spectral analysis to identify useful emission lines to monitor the welding process [52].

Zhiyong et al. [53] studied the changes in spectrum identifying spectral zones that act as indicators to detect defects in situ in GTAW process. It was observed that by introducing disturbance factors such as oil, rust, cross air puffing, and variation of welding speed resulted in the change in composition of plasma gases. This led to increased peaks correlating to certain elements in the

spectrum, thus indicating the effect of a disturbance factor. The effect of the oxide layer on a lap joint faying surface of magnesium sheets was studied by Harooni et al. [54] by analyzing spectrum signals captured during laser welding. The study revealed that the presence of the magnesium oxide layer leads to porosity defect at the interface of the joint. It was found that the removal and preheating of this layer resulted in a reduced number of pores at the interface. Further validation was done by analyzing images captured using a charge coupled device (CCD) camera and deriving the electronic temperature profiles.

Spectral signals have also been analyzed using statistical methods in combination with neural networks to identify weld defects. Mirapeix et al. [55] proposed a novel method to detect and classify weld defects with PCA and ANNs. The redundant information in plasma spectra captured during the welding process is removed using PCA, thereby reducing the dimensions of the feature space. A portion of the resulting data was fed to train the multilayer feed-forward neural network. Furthermore, the trained network was used to classify the test data into lack of penetration, low welding current, inert gas flow reduction, and correct welding. These results were validated with experimental electronic temperature profiles.

You et al. [56] presented a model that proved that complex industrial-scale sensors could be replaced by simple laboratory sensors to monitor the welding process and defect detection. The model used both a photodiode and spectrometer to acquire data. The data was then subjected to PCA, and the resulting features were used to train a support vector machine (SVM) model that classifies welding defects. The mean classification accuracy of the proposed model is 81.34%, while the accuracy reported using laboratory-scale sensors is 78.30%.

PCA of spectral signals has also been used in conjunction with EMD for detecting porosity and studying the effect of sheet gap on its formation [57]. PCA was used to select the spectral band of interest, followed by an improved K-medoids clustering algorithm [58] to select the spectral lines. EMD was applied to the intensity ratio on hydrogen and argon. It was observed that increasing the gap decreases porosity formation; however, increasing the gap beyond 0.9 mm could lead to the formation of burn-off flaws.

To address the drawbacks of using PCA especially the lack of interpretability, Mirapeix et al. [59] proposed an alternative redundancy removal algorithm called sequential forward floating selection (SFFS). The use of SFFS explained the association between the selected spectral bands and emission lines of the chemical species involved in plasma. The algorithm reduced the feature space to much lower dimensions than achieved by PCA. The compressed data after eliminating redundancies was used to train the neural network.

Other statistical parameters like the root mean square signal of the welding plasma spectra of the chosen emission lines from the spectrum have been used to monitor the weld quality and locate defects [60]. The observations made with RMS signals were backed by evidences in heat input profiles, obtained by the product of RMS values of voltage and current divided by the welding speed and the wavelength associated with maximum intensity of the plasma.

An algorithm using the CUSUM (or cumulative sum) least square filter on chosen spectral line data to detect weld defects was suggested by Daniel et al. [61]. The plasma spectral data of the selected emission lines was collected by capturing the perturbations introduced in the electric arc, varying welding current, welding speed, and shielding gas flow rate. The algorithm was applied on the signals of the spectral signal with resulting peaks indicating the presence of defects.

Zhang et al. [62] presented a methodology using plasma spectroscopy signal to detect hydrogen-induced porosity defect. The emission lines corresponding to hydrogen and argon were selected as they are part of the weld plasma, and six features were extracted from the spectral signals. A threshold-based selection of features was carried out using Fisher distance criteria. The peak area ratio between hydrogen and argon was selected as the monitoring parameter due to its high sensitivity towards porosity. Two features with the highest Fisher distance were used to train the SVM classifier that classifies the weld samples into good and defective welding classes.

Spectroscopic analysis is an optical method which provides intuitive information regarding the welding process. Concrete correlations can be established between the spectral peaks and weld arc properties. A more rudimentary method of visual analysis involves directly analyzing the images recorded during the process for defect detection and monitoring.

### 3.2 Vision sensing

Vision sensing involves recording the weld process using a high speed camera and analyzing them using computer vision-based methods to identify any deviations from ideal conditions for the detection of defects. This analysis can be performed by feeding large amounts of data to CNNs either directly or after applying filters. Gaussian filtering on welding arc images was performed by Agus et al. [8], to train a custom CNN architecture. The trained classifier reported a test accuracy of 95.83% in classifying the three welding defects, viz., spatter, porosity, and undercut.

Daniel et al. [63] conducted a thorough investigation on the performance of several fully connected neural network (FCN) architectures and CNN architectures by varying the hyperparameters such as learning rate, batch size, and the

number of epochs to classify the welding arc images into two classes of good and bad weld images, or into more complex four class or six class classifiers. The CNNs outperformed the FCNs in classifying the arc images. The accuracies reported were as high as 95%. Zhang et al. [64] demonstrated the use of a non-zero pixel method to evaluate the feature learning ability of CNN and to further decide the number of layers and filters in each layer of the network. The performance of the trained CNN model was further boosted by augmenting the dataset that contained welding arc images capturing the weld pool from different angles.

Xia et al. [65] used the center loss metric along with softmax loss function to optimize the ResNet18 model [66]. This trained model achieved a test accuracy of 98% in classifying the arc welding images. The authors also visualized the features learned by the deep learning model using the Guided Grad-CAM algorithm and thereby interpreting their physical meaning. Vision sensing is often computationally intensive. Therefore, enough computational power is required to make these methods suitable for in situ monitoring. However, the data collected via vision sensing is easily interpretable. An alternative method of vision sensing that involves capturing the thermal images of data is covered in the following section.

### 3.3 Infrared thermography

Weld defects can also be detected by analyzing the thermal images recorded during the process. Studies reported that IR thermography was useful in monitoring the friction welding process [67]. Alfaro et al. [68] explored the possibility of using an infrared sensor to detect defects in the arc welding process. It was observed that the mean value of the infrared signal data indicated the depth of weld penetration, and the perturbations in the AC portion of the signal corresponded to the irregularities in the surface of the bead. A change detection method was proposed using the Kalman filter to set a threshold on the Mahalanobis distance of the filtered data to detect the presence of defects.

Its viability for friction stir welding was also demonstrated by Kryukov et al. [69] for detection of defects such as wormholes, lack of penetration, and lack of fusion. Cooling sequence images of each component of the friction stir weld were obtained by extracting the column-wise data of each interval in each image, thereby acquiring a sequence of images at each interval of the entire object of interest. They showed that imperfections as small as 1.5 mm could be detected using thermograms.

IR thermography has also found applications in additive manufacturing techniques. It has been used for in situ monitoring of laser metal deposition [70]. It therefore can be exploited for defect detection in a variety of methods apart from traditional welding. While images are usually multi-dimensional, other 1-D signals like welding current and voltage can be observed to identify aberrations in welding.

## 4 Defect detection using welding current and voltage signals

The welding current and voltage signals recorded during welding operation are reliable indicators of arc stability and help to identify defects in the weld bead. Several studies have used statistical analysis of welding current and voltage signals. Others have used deep neural network (DNN) architectures and feature extraction to monitor the welding process.

Adolfsson et al. [71] used statistical parameters like variance of the welding current and voltage signals and subjected the data to sequential probability ratio rest (SPRT). The variance of welding current and voltage showed robustness in detecting the disturbances caused by the step defect which was introduced by using a T-joint in which gaps had been cut out from the standing plate. A decrease in the maximum short circuit frequency was also observed when the welding parameters deviated from ideal conditions.

Sumesh et al. [72] established a correlation between weld defects and welding current and voltage signatures. Due to the highly transient nature of these signals, their probability density distributions (PDD) served as indicators of weld defects like porosity and burn through. Porosity was introduced through different methods: applying grease, beaming air, and switching off shielding gas. The PDD of the undisturbed arc had three peaks indicating the peak, shoulder, and background currents. The transient current signals observed during porosity were characterized by the ramping current waveform rather than a sudden increase; this was also evident in the PDD plots. The voltage PDD had lower values and a flat region, which signified a drop in voltage during short-circuiting. These observations were similar in all three methods of introducing porosity. The PDD plots varied greatly from those of perfect welding, thus giving strong indications that the PDD plots are reliable indicators of weld defects.

Simpson et al. [73] presented a novel method of using welding current and voltage data to create signature images; signature images are similar to histogram plots with the additional advantages of improved resolution for particular bins. The voltage and current values are scaled, and an error function is used to change their range to [0, 1]. They also used a fuzzy logic approach where a particular bin's point also contributed to containers nearby. The Euclidean distance of the signature images from the mean of all the perfect welds was used as a parameter for classifying the weld as perfect or imperfect.

The variations in statistical parameters were also used by Wu et al. [74]. The variations were observed by introducing a step disturbance in the weld bead. Several parameters like mean, standard deviation, kurtosis, and coefficient of variation were calculated from the data obtained. Using a control chart, the upper and lower control lines were calculated. The welding data confined within these control lines was identified as proper welding while the data which deviated were marked as irregularities.

Madigan et al. [75] put forward a method using arc sensing to identify defects in constant voltage GMAW. The work used seven algorithms for determining the defects, which are running average and standard deviation of welding current-voltage and resistance (obtained by dividing voltage and current), arc condition number (a measure of low-frequency stability of the process), the current trend, the voltage trend, the short circuit frequency, and its standard deviation. Based on these values, quality parameters were calculated to set the thresholds for classifying the welds. The algorithms were tested for sensitivity, and the defect detection algorithms were evaluated. It was found that the quality parameters were sensitive to lack of shielding gas, dirty parts, and melt through. The rise in arc condition was correlated to disturbances due to oil which caused subsurface porosity. The work also noted that although the above parameters were useful, they were not sensitive to all defects.

Rehfeldt et al. [76] used an unsupervised learning algorithm, the Kohonen network [77], to automatically classify the defects. Like other approaches, it uses PDD of weld voltage and class frequency distribution (CFD) of the short-circuiting time as input vectors to the neural network. The network is made up of a 2-D neuron configuration. The trained Kohonen network exhibited an accuracy of 92%. One of the main benefits of using an unsupervised learning algorithm is that it eliminates the need for an expert to monitor and interpret the different PDDs.

Huang et al. [78] came up with a time-frequency domain analysis to identify weld defects. The research uses an improved version of EMD known as complete ensemble empirical mode decomposition with adaptive noise (CEEMDAN). After the IMFs are calculated using CEEMDAN, each of the frequency bands has varied energies. The entropies of the first eight normalized IMFs are given as the input feature vector to the extreme learning machine [79]. The extreme learning machine is based on the idea that a single-layer neural network can learn faster and generalize better than regular neural networks. The output is a multi-label classification vector that classifies the weld into surface porosity, poorly formed pattern, well-formed pattern, and a wider weld.

Feature extraction from welding current and voltage signals for identifying was presented by Zhang et al. [80]. Wavelet packet transform was used to remove pulse interference and noise. The Welch method [81] was used to perform frequency domain analysis and plot the power spectrum distribution of the collected data. RMS of the various frequency bands displayed varying sensitivity to the weld defects. The algorithms successfully identified flaws like lack of penetration and burn through.

Huang et al. [82] observed a strong correlation between the plasma electric signals and weld quality. The denoised signal was reconstructed after removing high-frequency components using wavelet packet transformation. Ensemble empirical mode decomposition (EEMD) was applied on the denoised signal to extract the useful frequency component and to retain most of the information. The fluctuations and ranges of residual voltage waveforms indicated the presence of surface defects. Recent studies have explored using deep learning techniques for porosity detection using welding current and voltage signals [83]. These signals usually have a direct impact on the welding arc. Often, any deviations in arc behavior are reflected clearly in the these signals. The accuracies of defect detection can be improved when these signals are used in conjunction with other input signals.

## 5 Multi-sensor-based defect detection

The preceding sections presented a review of weld defect detection using a single type of input signal, i.e., acoustic, optical, or welding current and voltage signals. However, the robustness and reliability of defect detection can be enhanced by using models that can efficiently combine information from multiple signals. This approach helps us correlate observations inferred from different signals and predict the quality of the weld with much better accuracy.

Zhang et al. [84] presented a model that used features extracted from voltage, sound, and spectrum signals. Relative wavelet energies of lower frequency bands of sound data, RMS of negative half-wave of arc voltage data, and the variance of argon emission line were chosen as they were most sensitive to change in seam penetration. The upsampling method was used to bring size-synchronization among the features extracted from data of various sensors. The fused data was used to train the SVM-based 10-fold cross-validation classifier. The proposed model reported a test accuracy of 96.6%, while single-sensor-based models reported 92%, 74%, and 77%, proving that the multi-sensor-based model performs better than a single-sensor-based model.

Zhang et al. [85] also proposed an improved multi-sensor-based method that utilizes the sound and voltage data used for weld monitoring and spectrum signal to detect defects such as porosity. The spectrum signal was downsampled to match the size of voltage and sound data. Statistical features such as kurtosis, variance, and RMS were extracted

from the voltage and sound data, and the variance ratio of hydrogen and argon was obtained from the spectrum signal data. Filter-based methods rank the features and select the features with high scores, whereas the wrapper-based methods score the features depending on the learning algorithm's performance. The Fisher distance-based filter method was employed to select high-ranked features, and the wrapper-based approach, along with support vector machine-grid search and cross-validation (SVM-GSCV), was used to select a subset of features that best classifies the defects. The model achieved a classification accuracy of 94.7% after removing the redundant information by using the proposed hybrid feature selection method.

A similar classification model that uses features extracted from arc voltage, audible sound, and spectrum signal was presented by Zhang et al. [86]. The features extracted include RMS and variance values of several spectral bands of interest in the spectrum signal, RMS, and kurtosis values of the sound signal in the time domain and frequency domain and RMS, kurtosis, and other statistical features of the positive and negative half cycles of the arc voltage signal. The spectrum signal features gave the best performance among the single-sensor models while classifying normal welding, burn through, and under-penetration. The performance of the two sensor models was comparable. However, the multi-sensor-based SVM classification model reported an accuracy of 94.5% , which declined to 93.4% after the feature dimension reduction.

Deng et al. [87] proposed a CNN for in-process defect detection for laser welding called IDDNet which utilized a multi-sensor data fusion network. The model uses the time series data of plasma intensity, light intensity, and temperature data to classify samples into nine classes, including missing weld defect. The network achieved an overall classification accuracy of above 90%, and the model was implemented in a real-time industrial environment on a single GTX 1080ti graphics card. A laser welding monitoring setup consisting of a pyrometer, two photodiode sensors, and other optical components was proposed, and it was integrated into the laser welding machine for capturing real-time data.

Though multi-sensor fusion has the advantage of improved accuracy, it also adds the additional burden of increased costs and need for more computational power. This trade-off needs to be considered while implementing these methods in real time. Multi-sensor approaches can be paired with feature reduction methods to decrease the computational load by getting rid of redundant features.

## 6 Classification of algorithms for defect detection

Given the variety of features used in weld defect detection, numerous algorithms have been proposed to process the features and identify defects. Specific features might often work better with particular algorithms to achieve best accuracy. It is also advisable to have an overall idea of the prominent algorithms which have found wide applications in weld defect detection, to have better knowledge to know which algorithm is best suited for a particular situation. The current section describes the methods employed for the extraction of features and classification of defects. These methods can be classified into three broad categories: signal processing–based methods, statistical feature extraction methods, and machine learning–based approaches as illustrated in Fig. 9.

### 6.1 Signal processing–based algorithms

Short-time Fourier transform [88], wavelet transform [89], EMD [90], and its variants such as EEMD [91] and CEEMDAN [92] are frequently used time-frequency analysis techniques. Short-time Fourier transform [88] divides the signal into equal segments and performs Fourier transform, thereby retaining both time and frequency domain information [93, 94]. However, the uncertainty principle of signal analysis indicates that there is a time-frequency resolution trade-off.

Wavelet transform is similar to Fourier transform, but it mainly differs in the merit function used for decomposing the signal. Fourier transform decomposes a signal into sines and cosines, whereas the wavelet transform uses merit functions localized in both time and frequency domain such as Daubechies [89, 95, 96], Haar, Morlet, and many more. Utilizing the scaling and shifting properties of the wavelet functions, wavelet transform decomposes the signal into several frequency bands, improving the

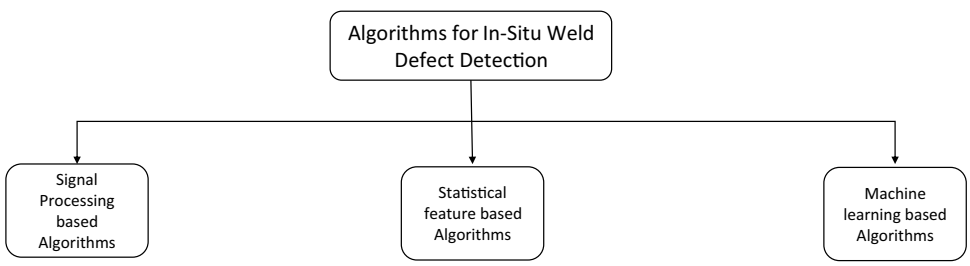


**Fig. 9** Schematic representation of various algorithms used for in situ weld defect detection

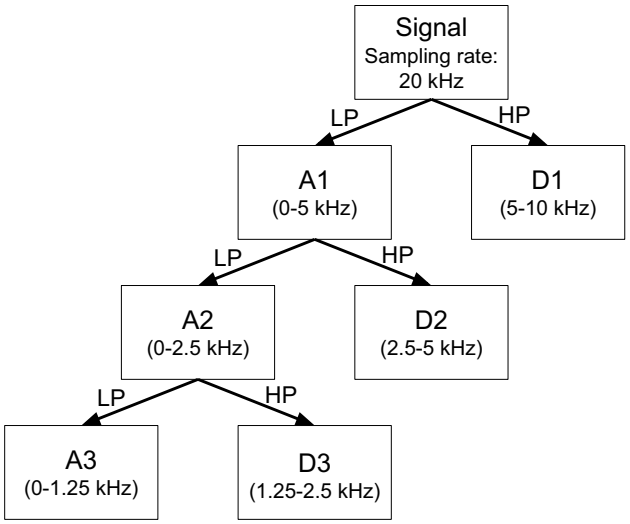


**Fig. 10** Illustrative representation of 3-level wavelet decomposition

time-frequency resolution over the Fourier analysis while retaining the time domain information. Discrete wavelet transform decomposes the signal into approximate ($A_n$) and detail signals ($D_n$) passing the signal through a series of low pass (LP) and high pass (HP) filters as shown in Fig. 10. Readers may refer to Shensa [97] for a detailed description of the discrete wavelet transform.

EMD is a technique of decomposing the signal into a set of IMFs in the time domain without any basis function [90]. An IMF satisfies the condition that the number of extrema and zero crossings differ at most by one, and the mean value of the envelope defined by local maxima and envelope defined by local minima is zero at any instant. These conditions allow us to define instantaneous frequency to the IMFs, which can be highlighted by applying the Hilbert transform. EMD is commonly applied to analyze seismic graphs, electrocardiograms, and many such non-stationary signals.

The sequence of steps involved in arriving at the IMFs (Fig. 11) is as follows:

- Obtain the local extrema and minima of the time series signal $x(t)$.
- Plot the local extrema to obtain the upper envelope $\max(x(t))$ and the local minima to obtain the lower envelope $\min(x(t))$.
- Find the mean of the upper and lower envelopes.

$$\text{mean}(x(t)) = \frac{\max(x(t)) - \min(x(t))}{2} \tag{1}$$

- Subtract the mean from the original signal to extract the IMF of the signal.
- Iterate this process with the residue signal until the stoppage criterion is satisfied:

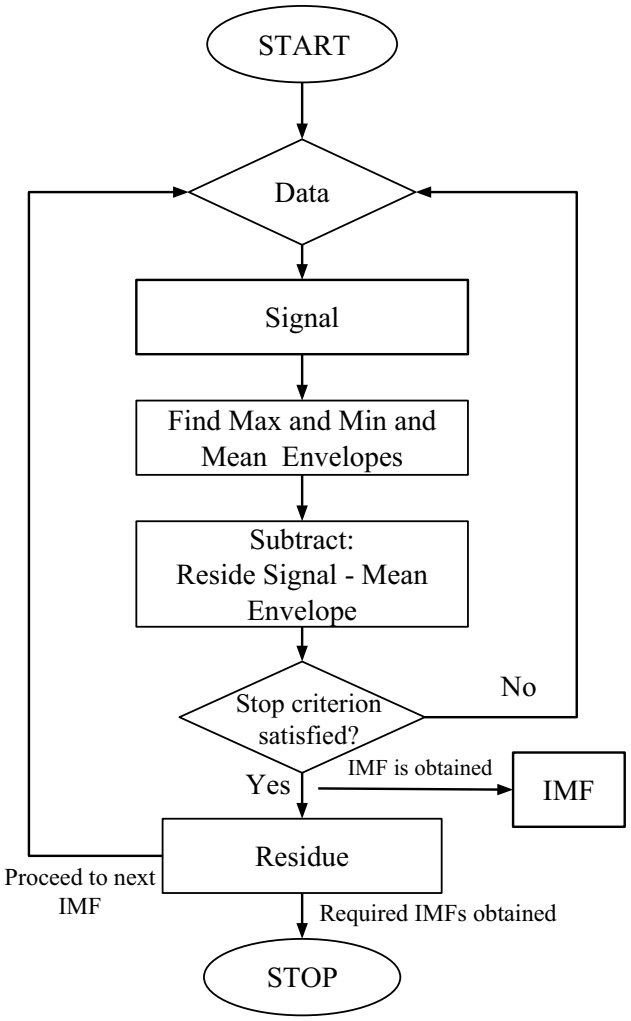


**Fig. 11** Process flow diagram of EMD algorithm

$$\text{residue signal} = \text{original signal - IMF} \tag{2}$$

To overcome the drawback of mode mixing in EMD, Wu and Huang [91, 98] proposed a noise-assisted EMD approach known as the EEMD. It involves adding different white series noise to the original signal in each trial and taking the ensemble average of the intrinsic mode functions obtained over several trials. The addition of noise makes the IMF in one trial uncorrelated to IMFs in other trials, thus removing the effect of mode mixture and separating time scales.

However, when the number of trials is meager, the extracted IMFs are contaminated by noise. To reduce this problem, Yeh and Huang [99] proposed the addition of paired noises with positive and negative signs, compensating the residual noise while reconstructing the original signal. This method is known as CEEMD. Furthermore, Torres [92, 100] proposed complete ensemble empirical mode

decomposition with adaptive noise (CEEMDAN) in which the residual white noises are extracted from the mixture of data and additive white noise using complementary ensemble IMFs with positive and negative added white noise. While conventional signal processing algorithms are more involved, often, statistical feature–based algorithms covered in the following section provide a simpler and straightforward approach.

### 6.2 Statistical feature–based algorithms

Statistical features such as RMS and kurtosis were reported as good indicators of defects. Dividing the fourth moment of distribution by the square of variance of input signal gives its kurtosis value. PDD is similar to a histogram giving the probability of occurrence of each range of values. Another prominent method which has found uses in weld defect detection is the CUSUM least square method [101].

Furthermore, dimensionality reduction is performed on the large number of features extracted by the ANNs from the data to reduce the computation time and remove the redundant information using PCA [102]. PCA involves finding the eigenvalues of the feature matrix and selecting features such that the variance is maximized and maximum energy of the eigenvalues is retained. Mirapeix [55] conducted a similar analysis to extract useful information from the spectral data.

The other frequently used dimensionality reduction technique is the Fisher linear discriminant (FLD). The main idea of Fisher-based method is to maximize the distance between data points of different classes and minimize the distance between the data points of the same class. Zhang [85] used the Fisher-based criteria to select useful features for the classification of defects. Often, in real-time defect monitoring, simple statistical features might not generalize well in giving the complete information about the defect. Machine learning approaches like ANNs have the ability to extract higher-level features taking these simpler features or the original signal itself as inputs.

### 6.3 Machine learning and deep learning approaches

Conventional machine learning algorithms include decision tree [103], SVM [104], and Naive Bayes [105]. In general, these methods use hand-engineered features, which require comprehensive domain knowledge for classification and regression tasks. These methods can extract only low-level features without hand-crafted features being fed into the models, resulting in poor accuracies.

The inspiration for neural networks was drawn from the human brain neurophysiology. The basic building block of neural networks is the perceptron [106]. A perceptron is a simple single-layer linear binary classifier that outputs the weighted sum of input features passed through an activation function. Neural networks [107], also known as multilayer perceptrons or feed-forward neural networks, generally have multiple hidden layers, with each layer having several neurons. These parameters are usually decided based on the amount of data in hand.

Traditional neural network learns the weights of each neuron and uses a non-linear activation function to map a complex relationship between input and output. However, CNNs [108] use convolution operation in place of matrix multiplication to learn the convolutional kernels' elements in each layer. Unlike the traditional machine learning algorithms, the CNNs do not require extensive domain knowledge for feature extraction. Rather, the CNNs can learn the features automatically from a large amount of raw training data through a back-propagation algorithm such as gradient descent. CNNs are usually applied on two-dimensional data, such as images, and features are extracted using alternating convolution and pooling layers. The more the hidden layers, the deeper the features extracted. The readers may refer to [109] for a more detailed description of neural networks.

Deep learning has taken a surge in recent times and has been deployed in diverse signal processing fields such as image processing, speech processing [110], medical imaging [111], and biomedical signal processing [112] due to its outperforming capabilities over conventional techniques. The use of greater number of layers in the neural network to extract higher-level features is termed as deep learning. Handling of the massive data and training of a tremendous number of parameters was further boosted by the recent advancements in parallel computing and with the use of GPUs and TPUs. Several landmark CNN architectures such as LeNet [113], VGG [114], GoogLeNet [115], and many more have been proposed for image classification in the past couple of decades. Numerous deep learning frameworks have been proposed in recent times, such as the recurrent neural networks (RNNs) [116] and general adversarial networks (GANs) [117]. 1D CNNs have come into use for modeling time series data like speech data. The utility of these recent neural network architectures in the aspect of in situ defect detection might be a topic of interest for future works in this area.

## 7 Discussion and conclusions

The preceding sections of this paper covered in situ weld defect detection by classifying it on the basis of input signals and the algorithms used along with intuitive explanations of a few widely used algorithms. The current section consolidates the data presented drawing inferences regarding the feasibility, advantages, disadvantages, and research gaps in the field of in situ weld defect detection. Figure 12

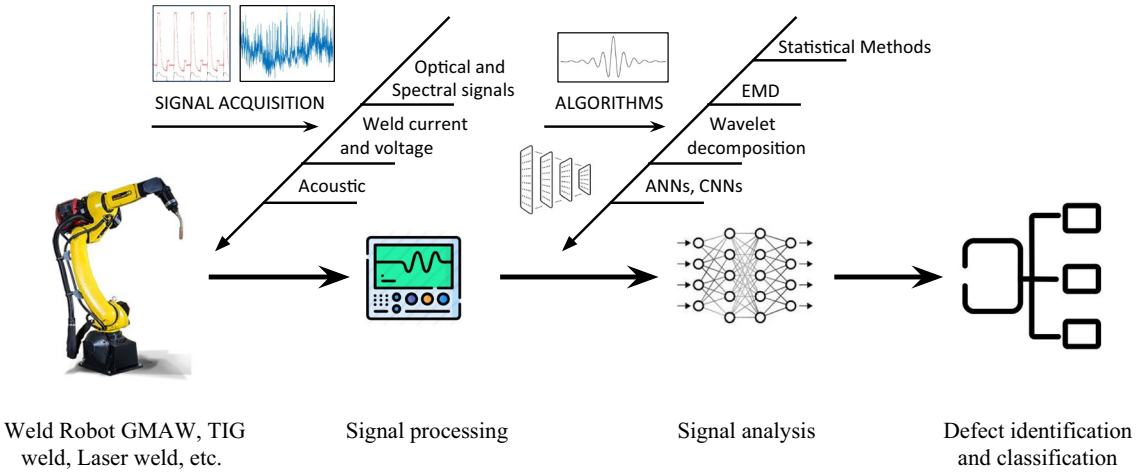


**Fig. 12** Process flow diagram for in situ classification of weld defects

illustrates the series of steps for in situ weld detection which starts with recording input signals using sensors, followed by their analysis using various algorithms which help in the identification and classification of defects.

To estimate the feasibility of a method, it is imperative to thoroughly analyze its advantages and disadvantages. In terms of ease of application, three main factors must be taken into consideration: reliability of signals, cost of implementation, and computational complexity. It can be noted that among various signals used for weld defect detection, audio-based approaches are simple and computationally less expensive. However, audio detection is prone to external disturbances, especially in the case of welding, which is usually performed in industrial environments, exposed to noise from other equipment. Statistical parameters like RMS and kurtosis, though indicators of defects, may vary with changes in parameters; therefore, a meticulous study of their behavior at various levels of input parameters is necessary for accurate prediction and classification. Going through various research works in acoustic signal monitoring, it can be inferred that rather than analyzing the audio data solely in the time or frequency domain, time-frequency analysis methods such as EMD and STFT provide useful information about the type and location of the defect. This analysis is instrumental because any deviation from ideal behavior is reflected by a change in the frequency components of the emitted audio signal; knowing the time instant of this change in frequency components helps to locate the defect with precision. Acoustic emissions are extremely sensitive and responsive and can be used to identify defects with greater accuracy than audio signals. These methods also involve reasonably lesser capital investments for setting up than radiographic setups which are costly and computationally intensive requiring computing facilities with high data processing abilities.

The welding current and voltage signals recorded during the process are highly reliable as they offer a direct glimpse into the actual process and weld cycles. Any change in the weld parameters is directly indicated by a change in the welding current and voltage signals. Statistical or spectral analysis of these signals is not computationally expensive; these methods can be used to analyze and identify defects without much delay. Since each weld reflects differently in the current-voltage signals, the defects can be located and classified with better accuracy.

Several papers identified that the spectral signals are good indicators of defects that involve the change in the composition of ionized gases in the plasma. Defects such as porosity occur due to the presence of gas bubbles trapped on the weld piece. Spectrum signals often capture these changes in the plasma composition and reflect in some statistical parameters when analyzed, thereby being a reliable indicator of porosity and several such defects.

Machine learning and deep learning models are especially advantageous because they are exposed to large amounts of training data, thus ensuring that they are capable of detecting more varieties of defects with better accuracy. Since ANNs usually learn the weights on their own, this simplifies the tasks to be done by the user; the network can be fed with simple statistical features or the audio signal itself. ANNs and deep learning approaches usually fare better than traditional methods in modeling complex relationships between parameters which is often the case in welding.

Weld penetration depth and spatter are found to be reflected in the welding current and voltage signals, and porosity can be detected using spectrum signals; surface defects such as cracks can be identified by analyzing weld

**Table 1** Utility of various signals for identifying different types of weld defects

| Input signal | Defects detected using the acquired signal |
|---|---|
| Audible sound | Porosity [37, 39]; burn through [36, 40] |
| Acoustic emission | Porosity and cracks [47]; burn through [45] |
| Spectroscopy | Porosity [57, 62]; lack of penetration [55, 60] |
| Images | Porosity and spatter [8]; undercut [65]; burn through [64]; lack of fusion [63] |
| IR thermography | Wormholes and lack of fusion [69]; undercuts and blowouts [56] |
| Welding current and voltage | Porosity [57, 72, 78, 83] |

arc images. Surface defects and depth monitoring can be achieved by analyzing the welding arc images. The conventional image processing techniques do not generalize well in the practical scenario due to occlusion and other noises. CNNs are suitable in such cases as they can extract deeper features from the data. However, the training of the deep learning models is a computationally intensive task, making the hardware implementation more challenging. Simpler and lightweight architectures like MobileNet [118] and ShuffleNet [119] have been used in various applications due to their low computational power requirement. Deng [87] proposed a relatively shallower CNN architecture known as IDDNet, which has been deployed onto a single GTX 1080ti graphics card. Feature extraction and classification of defects can be carried out by applying the recently proposed 1D CNNs [120] on the acoustic, spectrum, welding current, and welding voltage data, thereby reducing the computational complexity as the number of trainable parameters of 1D CNNs are relatively lower than that of 2D CNNs.

Presently the number of methods capable of multi-class defect detection is scarce. A plausible explanation for this is that some defects are easier to detect than others. It is plausible that some signals may not be susceptible to changes due to particular types of defects, while they may clearly indicate others. It is evident from Table 1 that several researchers have explored porosity and similar defects in great detail; future work needs to be directed towards studying a greater range of defects. A single-sensor data cannot be sufficient to detect multiple defects; hence, there is a need for multi-sensor data fusion methods which bear the advantages and characteristic features of each sensor data. There are very few models capable of multi-defect classification. Most works in the area of weld defect classification have focused on one particular defect and its effect on the parameters of interest. It is seldom the case in real-time welding that only one particular defect will occur. More comprehensive studies are required towards multi-defect classification. Most of the work in this regard offer theoretical evidence correlating the parameters with weld defects or highlighting the feasibility of a particular signal for weld defect detection. However, research works which have actually implemented these models in real time are scarce.

Although many research groups have been working on defect detection in welding, publicly accessible experimental datasets of welding sound, current, voltage, or images are still unavailable. Access to a dataset is often a barrier for several researchers. The presence of a publicly available dataset will fuel the development of new deep learning models that will further improve classification accuracies. A universally available dataset will also enable transfer learning where models can be trained for real-time applications with lesser amount of data.

A lot of ambiguity still exists on the type of defect to be studied and how the defects are introduced. A consensus is required on a common set of defects and methods for their realistic introduction during the welding process so that different research works and results can be compared. This will also improve the interchangeability of methods, equipping researchers with the ability of confidently applying an already existing method to their application. The ability of in situ weld defect detection algorithms to be extended to similar methods like metal additive manufacturing can be a potential area for future research. Not limiting these techniques to defect identification alone, studying the efficacy and feasibility of these techniques to predict properties of the finished weld bead while the welding process is going on could potentially save numerous hours which are lost in quality analysis post manufacturing. Research towards in situ detection still has several avenues which have not been yet tapped into. The research towards these areas, specifically real-time implementation in the industry, will potentially help save thousands of hours in post-processing of weld components while additionally boosting productivity and improving output quality.

**Acknowledgements** The authors gratefully acknowledge the support of the Science and Engineering Research Board, Department of Science and Technology, Government of India under the Ramanujan Research Grant (Grant number: SB/S2/RJN-093/2015) and Core Research Grant (CRG/2020/005089); authors also acknowledge the support of the Naval Research Board (NRB/4003/PG/436).

**Author contributions** Anirudh Sampath Madhvacharyula: Conceptualization, methodology, formal analysis, writing original draft, and visualization

Araveeti V Sai Pavan: Conceptualization, methodology, formal analysis, writing original draft, and visualization

Subrahmanyam Gorthi: Conceptualization, methodology, supervision, formal analysis, writing - review and editing, and visualization

Srihari Chitral: Conceptualization, methodology, formal analysis, writing original draft, and visualization

N. Venkaiah: Conceptualization, methodology, supervision, formal analysis, writing - review and editing, and visualization

Degala Venkata Kiran: Conceptualization, methodology, resources, supervision, formal analysis, writing - review and editing, visualization, project administration, and funding acquisition

**Funding** This work was supported by the Science and Engineering Research Board, Department of Science and Technology, Government of India under the Ramanujan Research Grant (Grant number: SB/S2/RJN-093/2015) and Core Research Grant (CRG/2020/005089). Authors also acknowledge the support of Naval Research Board (NRB/4003/PG/436).

**Availability of data and material** Not applicable.

**Code availability** Not applicable.

## Declarations

**Conflict of interest** The authors declare no competing interests.

**Ethics approval** Not applicable.

**Consent to participate** Not applicable.

**Consent for publication** The authors give their consent for the publication of the submitted manuscript in the journal *International Journal of Advanced Manufacturing Technology*.

## References

1. Kalpakjian S (1984) Manufacturing processes for engineering materials. Pearson Education India. https://doi.org/10.1007/BF02833667
2. Matsunawa A, Mizutani M, Katayama S, Seto N (2003) Porosity formation mechanism and its prevention in laser welding. Welding International 17(6):431–437. https://doi.org/10.1533/wint.2003.3138
3. Kam DH, Lee TH, Kim DY, Kim J, Kang M (2021) Weld quality improvement and porosity reduction mechanism of zinc coated steel using tandem gas metal arc welding (GMAW). Journal of Materials Processing Technology:117127, https://doi.org/10.1016/j.jmatprotec.2021.117127
4. Beidokhti B, Dolati A, Koukabi A (2009) Effects of alloying elements and microstructure on the susceptibility of the welded HSLA steel to hydrogen-induced cracking and sulfide stress cracking. Materials Science and Engineering: A 507(1–2):167–173. https://doi.org/10.1016/j.msea.2008.11.064
5. Hanzaei AT, Marashi SPH, Ranjbarnodeh E (2018) The effect of hydrogen content and welding conditions on the hydrogen induced cracking of the api x70 steel weld. International Journal of Hydrogen Energy 43(19):9399–9407. https://doi.org/10.1016/j.ijhydene.2018.03.216
6. Javadi Y, Sweeney NE, Mohseni E, MacLeod CN, Lines D, Vasilev M, Qiu Z, Mineo C, Pierce SG, Gachagan A (2021) Investigating the effect of residual stress on hydrogen cracking in multi-pass robotic welding through process compatible non-destructive testing. Journal of Manufacturing Processes 63:80–87. https://doi.org/10.1016/j.jmapro.2020.03.043
7. Shafeek H, Gadelmawla E, Abdel-Shafy A, Elewa I (2004) Automatic inspection of gas pipeline welding defects using an expert vision system. NDT & E International 37(4):301–307. https://doi.org/10.1016/j.ndteint.2003.10.004
8. Khumaidi A, Yuniarno EM, Purnomo MH (2017) Welding defect classification based on convolution neural network (CNN) and gaussian kernel. In: 2017 International seminar on intelligent technology and its applications (ISITIA), IEEE, pp 261–265. https://doi.org/10.1109/ISITIA.2017.8124091
9. Chu HH, Wang ZY (2016) A vision-based system for post-welding quality measurement and defect detection. The International Journal of Advanced Manufacturing Technology 86(9):3007–3014. https://doi.org/10.1007/s00170-015-8334-1
10. Zolfaghari A, Zolfaghari A, Kolahan F (2018) Reliability and sensitivity of magnetic particle nondestructive testing in detecting the surface cracks of welded components. N 33(3):290–300, https://doi.org/10.1080/10589759.2018.1428322
11. Lopez AB, Santos J, Sousa JP, Santos TG, Quintino L (2019) Phased array ultrasonic inspection of metal additive manufacturing parts. Journal of Nondestructive Evaluation 38(3):1–11. https://doi.org/10.1007/s10921-019-0600-y
12. Buckley J, Servent R (2009) Improvements in ultrasonic inspection of resistance spot welds. Insight-Non-Destructive Testing and Condition Monitoring 51(2):73–77
13. Passini A, Oliveira ACd, Riva R, Travessa DN, Cardoso KR (2011) Ultrasonic inspection of AA6013 laser welded joints. Materials Research 14(3):417–422. https://doi.org/10.1590/S1516-14392011005000057
14. Hwang YI, Park J, Kim HJ, Song SJ, Cho YS, Kang SS (2019) Performance comparison of ultrasonic focusing techniques for phased array ultrasonic inspection of dissimilar metal welds. International Journal of Precision Engineering and Manufacturing 20(4):525–534. https://doi.org/10.1007/s12541-019-00085-1
15. Moles M, Dubé N, Labbé S, Ginzel E (2005) Review of ultrasonic phased arrays for pressure vessel and pipeline weld inspections. Journal of Pressure Vessel Technology. https://doi.org/10.1115/1.1991881
16. Dorafshan S, Maguire M, Collins W (2018) Infrared thermography for weld inspection: feasibility and application. Infrastructures 3(4):45. https://doi.org/10.3390/infrastructures3040045
17. Broberg P, Runnemalm A (2012) Detection of surface cracks in welds using active thermography. In: 18th World conference on nondestructive testing. Durban, South Africa, pp 16–20
18. Li T, Almond DP, Rees DAS (2011) Crack imaging by scanning pulsed laser spot thermography. NDT & E International 44(2):216–225. https://doi.org/10.1016/j.ndteint.2010.08.006
19. Schlichting J, Brauser S, Pepke LA, Maierhofer C, Rethmeier M, Kreutzbruck M (2012) Thermographic testing of spot welds. NDT & E International 48:23–29. https://doi.org/10.1016/j.ndteint.2012.02.003
20. Meola C, Carlomagno GM, Squillace A, Giorleo G (2004) The use of infrared thermography for nondestructive evaluation of joints. Infrared physics & Technology 46(1–2):93–99. https://doi.org/10.1016/j.infrared.2004.03.013
21. Todorov E, Nagy B, Levesque S, Ames N, Na J (2013) Inspection of laser welds with array eddy current technique. AIP Conference Proceedings, American Institute of Physics 1511:1065–1072. https://doi.org/10.1063/1.4789161
22. Rao B, Raj B, Jayakumar T, Kalyanasundaram P (2002) An artificial neural network for eddy current testing of austenitic stainless steel welds. NDT & E International 35(6):393–398. https://doi.org/10.1016/S0963-8695(02)00007-5

23. Dmitriev S, Malikov V, Sagalakov A, Shevtsova L (2017) Flaw inspection of welded joints in titanium alloys by the eddy current method. Welding International 31(8):608–611. https://doi.org/10.1080/09507116.2017.1295563
24. Nadzri NA, Ishak M, Saari MM, Halil AM (2018) Development of eddy current testing system for welding inspection. In: 2018 9th IEEE Control and system graduate research colloquium (ICSGRC), IEEE, pp 94–98. https://doi.org/10.1109/ICSGRC.2018.8657511
25. Gao P, Wang C, Li Y, Cong Z (2015) Electromagnetic and eddy current NDT in weld inspection: a review. Insight-Non-Destructive Testing and Condition Monitoring 57(6):337–345. https://doi.org/10.1784/insi.2015.57.6.337
26. Hou W, Zhang D, Wei Y, Guo J, Zhang X (2020) Review on computer aided weld defect detection from radiography images. Applied Sciences 10(5):1878. https://doi.org/10.3390/app10051878
27. Kasban H, Zahran O, Arafa H, El-Kordy M, Elaraby SM, Abd El-Samie F (2011) Welding defect detection from radiography images with a cepstral approach. NDT & E International 44(2):226–231. https://doi.org/10.1016/j.ndteint.2010.10.005
28. Vilar R, Zapata J, Ruiz R (2009) An automatic system of classification of weld defects in radiographic images. NDT & E International 42(5):467–476. https://doi.org/10.1016/j.ndteint.2009.02.004
29. Zahran O, Kasban H, El-Kordy M, Abd El-Samie F (2013) Automatic weld defect identification from radiographic images. NDT & E International 57:26–35. https://doi.org/10.1016/j.ndteint.2012.11.005
30. Lopez A, Bacelar R, Pires I, Santos TG, Sousa JP, Quintino L (2018) Non-destructive testing application of radiography and ultrasound for wire and arc additive manufacturing. Additive Manufacturing 21:298–306. https://doi.org/10.1016/j.addma.2018.03.020
31. Javadi Y, MacLeod CN, Pierce SG, Gachagan A, Lines D, Mineo C, Ding J, Williams S, Vasilev M, Mohseni E et al (2019) Ultrasonic phased array inspection of a wire arc additive manufactured (WAAM) sample with intentionally embedded defects. Additive Manufacturing 29:100806. https://doi.org/10.1016/j.addma.2019.100806
32. Saini D, Floyd S (1998) An investigation of gas metal arc welding sound signature for on-line quality control. Welding Journal 77:172–s
33. Grad L, Grum J, Polajnar I, Slabe JM (2004) Feasibility study of acoustic signals for on-line monitoring in short circuit gas metal arc welding. International Journal of Machine Tools and Manufacture 44(5):555–561. https://doi.org/10.1016/j.ijmachtools.2003.10.016
34. Čudina M, Prezelj J, Polajnar I (2008) Use of audible sound for on-line monitoring of gas metal arc welding process. Metalurgija 47(2):81–85
35. Pal K, Bhattacharya S, Pal SK (2009) Prediction of metal deposition from arc sound and weld temperature signatures in pulsed MIG welding. The International Journal of Advanced Manufacturing Technology 45(11–12):1113. https://doi.org/10.1007/s00170-009-2052-5
36. Pal K, Bhattacharya S, Pal SK (2010) Investigation on arc sound and metal transfer modes for on-line monitoring in pulsed gas metal arc welding. Journal of Materials Processing Technology 210(10):1397–1410. https://doi.org/10.1016/j.jmatprotec.2010.03.029
37. Yusof M, Kamaruzaman M, Ishak M, Ghazali M (2017) Porosity detection by analyzing arc sound signal acquired during the welding process of gas pipeline steel. The International Journal of Advanced Manufacturing Technology 89(9–12):3661–3670. https://doi.org/10.1007/s00170-016-9343-4
38. Luo H, Zeng H, Hu L, Hu X, Zhou Z (2005) Application of artificial neural network in laser welding defect diagnosis. Journal of Materials Processing Technology 170(1–2):403–411. https://doi.org/10.1016/j.jmatprotec.2005.06.008
39. Pernambuco BSG, Steffens CR, Pereira JR, Werhli AV, Azzolin RZ, Estrada EdSD (2019) Online sound based arc-welding defect detection using artificial neural networks. In: 2019 Latin american robotics symposium (LARS), 2019 brazilian symposium on robotics (SBR) and 2019 workshop on robotics in education (WRE), IEEE, pp 263–268. https://doi.org/10.1109/LARS-SBR-WRE48964.2019.00053
40. Chatterjee S, Chatterjee R, Pal K, Pal S, Pal SK (2012) Accurate detection of weld defects using chirplet transform. In: International conference on computer and automation engineering, 4th (ICCAE 2012); ASME: New York, NY, USA, pp 49–54. https://doi.org/10.1115/1.859940.paper8
41. Mann S, Haykin S (1995) The chirplet transform: physical considerations. IEEE Transactions on Signal Processing 43(11):2745–2761. https://doi.org/10.1109/78.482123
42. Huang W, Kovacevic R (2009) Feasibility study of using acoustic signals for online monitoring of the depth of weld in the laser welding of high-strength steels. Proceedings of the Institution of Mechanical Engineers, Part B: Journal of Engineering Manufacture 223(4):343–361. https://doi.org/10.1243/09544054JEM1320
43. Roca AS, Fals HC, Fernández JB, Macías EJ, Adán FS (2007) New stability index for short circuit transfer mode in (GMAW) process using acoustic emission signals. Science and Technology of Welding and Joining 12(5):460–466. https://doi.org/10.1179/174329307X213882
44. Gu H, Duley WW (1996) A statistical approach to acoustic monitoring of laser welding. Journal of Physics D: Applied Physics 29(3):556
45. Zhang L, Basantes-Defaz AC, Ozevin D, Indacochea E (2019) Real-time monitoring of welding process using air-coupled ultrasonics and acoustic emission. The International Journal of Advanced Manufacturing Technology 101(5):1623–1634. https://doi.org/10.1007/s00170-018-3042-2
46. Asif K, Zhang L, Derrible S, Indacochea JE, Ozevin D, Ziebart B (2020) Machine learning model to predict welding quality using air-coupled acoustic emission and weld inputs. Journal of Intelligent Manufacturing:1–15. https://doi.org/10.1007/s10845-020-01667-x
47. Gaja H, Liou F (2017) Defects monitoring of laser metal deposition using acoustic emission sensor. The International Journal of Advanced Manufacturing Technology 90(1–4):561–574. https://doi.org/10.1007/s00170-016-9366-x
48. Kanungo T, Mount DM, Netanyahu NS, Piatko CD, Silverman R, Wu AY (2002) An efficient k-means clustering algorithm: analysis and implementation. IEEE transactions on pattern analysis and machine intelligence 24(7):881–892. https://doi.org/10.1109/TPAMI.2002.1017616
49. Roca AS, Fals H, Fernández J, Macias E, De La Parte M (2009) Artificial neural networks and acoustic emission applied to stability analysis in gas metal arc welding. Science and Technology of Welding and Joining 14(2):117–124. https://doi.org/10.1179/136217108X382981
50. Subramaniam S (2013) Acoustic emission-based monitoring approach for friction stir welding of aluminum alloy AA6063-T6 with different tool pin profiles. Proceedings of the Institution of Mechanical Engineers, Part B: Journal of Engineering Manufacture 227(3):407–416. https://doi.org/10.1177/0954405412472673
51. Chen C, Kovacevic R, Jandgric D (2003) Wavelet transform analysis of acoustic emission in monitoring friction stir welding of 6061 aluminum. International Journal of Machine Tools

and Manufacture 43(13):1383–1390. https://doi.org/10.1016/S0890-6955(03)00130-5
52. Griem HR (2005) Principles of plasma spectroscopy. 2, Cambridge University Press, https://doi.org/10.1007/978-94-017-0445-8_34
53. Zhiyong L, Bao W, Jingbin D (2009) Detection of GTA welding quality and disturbance factors with spectral signal of arc light. Journal of materials processing technology 209(10):4867–4873. https://doi.org/10.1016/j.jmatprotec.2009.01.010
54. Harooni M, Carlson B, Kovacevic R (2014) Detection of defects in laser welding of AZ31B magnesium alloy in zero-gap lap joint configuration by a real-time spectroscopic analysis. Optics and Lasers in Engineering 56:54–66. https://doi.org/10.1016/j.optlaseng.2013.11.015
55. Mirapeix J, García-Allende P, Cobo A, Conde O, López-Higuera J (2007) Real-time arc-welding defect detection and classification with principal component analysis and artificial neural networks. NDT & E International 40(4):315–323. https://doi.org/10.1016/j.ndteint.2006.12.001
56. You D, Gao X, Katayama S (2014) WPD-PCA-based laser welding process monitoring and defects diagnosis by using FNN and SVM. IEEE Transactions on Industrial Electronics 62(1):628–636. https://doi.org/10.1109/TIE.2014.2319216
57. Huang Y, Zhao D, Chen H, Yang L, Chen S (2018) Porosity detection in pulsed GTA welding of 5A06 Al alloy through spectral analysis. Journal of Materials Processing Technology 259:332–340. https://doi.org/10.1016/j.jmatprotec.2018.05.006
58. Park HS, Jun CH (2009) A simple and fast algorithm for k-medoids clustering. Expert Systems with Applications 36(2):3336–3341. https://doi.org/10.1016/j.eswa.2008.01.039
59. Garcia-Allende P, Mirapeix J, Conde O, Cobo A, Lopez-Higuera J (2009) Spectral processing technique based on feature selection and artificial neural networks for arc-welding quality monitoring. NDT & E International 42(1):56–63. https://doi.org/10.1016/j.ndteint.2008.07.004
60. Mirapeix J, Cobo A, Fuentes J, Davila M, Etayo JM, Lopez-Higuera JM (2009) Use of the plasma spectrum RMS signal for arc-welding diagnostics. Sensors 9(7):5263–5276. https://doi.org/10.3390/s90705263
61. Bebiano D, Alfaro SC (2009) A weld defects detection system based on a spectrometer. Sensors 9(4):2851–2861. https://doi.org/10.3390/s90402851
62. Zhang Z, Kannatey-Asibu E, Chen S, Huang Y, Xu Y (2015) Online defect detection of al alloy in arc welding based on feature extraction of arc spectroscopy signal. The International Journal of Advanced Manufacturing Technology 79(9):2067–2077. https://doi.org/10.1007/s00170-015-6966-9
63. Bacioiu D, Melton G, Papaelias M, Shaw R (2019) Automated defect classification of aluminium 5083 TIG welding using HDR camera and neural networks. Journal of Manufacturing Processes 45:603–613. https://doi.org/10.1016/j.jmapro.2019.07.020
64. Zhang Z, Wen G, Chen S (2019) Weld image deep learning-based on-line defects detection using convolutional neural networks for al alloy in robotic arc welding. Journal of Manufacturing Processes 45:208–216. https://doi.org/10.1016/j.jmapro.2019.06.023
65. Xia C, Pan Z, Fei Z, Zhang S, Li H (2020) Vision based defects detection for keyhole TIGwelding using deep learning with visual explanation. Journal of Manufacturing Processes 56:845–855. https://doi.org/10.1016/j.jmapro.2020.05.033
66. He K, Zhang X, Ren S, Sun J (2015) Deep residual learning for image recognition. https://doi.org/10.1109/CVPR.2016.90, arxiv:1512.03385
67. Serio L, Palumbo D, Galietti U, De Filippis L, Ludovico A (2016) Monitoring of the friction stir welding process by means of thermography. NDT & E International 31(4):371–383. https://doi.org/10.1080/10589759.2015.1121266
68. Alfaro SC, Franco FD (2010) Exploring infrared sensoring for real time welding defects monitoring in GTAW. Sensors 10(6):5962–5974. https://doi.org/10.3390/s100605962
69. Kryukov I, Schüddekopf S, Böhm S, Mund M, Kreling S, Dilger K (2016) Non-destructive online-testing method for friction stir welding using infrared thermography. In: 19th World conference on non-destructive testing
70. Hassler U, Gruber D, Hentschel O, Sukowski F, Grulich T, Seifert L (2016) In-situ monitoring and defect detection for laser metal deposition by using infrared thermography. Physics Procedia 83:1244–1252. https://doi.org/10.1016/j.phpro.2016.08.131
71. Adolfsson S, Bahrami A, Bolmsjö G, Claesson I (1999) On-line quality monitoring in short-circuit gas metal arc welding. Welding Journal-New York, 78:59–s
72. Sumesh A, Rameshkumar K, Raja A, Mohandas K, Santhakumari A, Shyambabu R (2017) Establishing correlation between current and voltage signatures of the arc and weld defects in GMAW process. Arabian Journal for Science and Engineering 42(11):4649–4665. https://doi.org/10.1007/s13369-017-2609-9
73. Simpson S (2007) Signature images for arc welding fault detection. Science and Technology of Welding and Joining 12(6):481–486. https://doi.org/10.1179/174329307X213909
74. Wu C, Gao J, Hu J (2006) Real-time sensing and monitoring in robotic gas metal arc welding. Measurement Science and Technology 18(1):303. https://doi.org/10.1088/0957-0233/18/1/037
75. Madigan R (1999) Arc sensing for defects in constant-voltage gas metal arc welding. Weld J 78:322S-328S
76. Wu C, Polte T, Rehfeldt D (2000) Gas metal arc welding process monitoring and quality evaluation using neural networks. Science and Technology of Welding and Joining 5(5):324–328. https://doi.org/10.1179/136217100101538380
77. Kohonen T, Honkela T (2007) Kohonen network. Scholarpedia 2(1):1568. https://doi.org/10.4249/scholarpedia.1568
78. Huang Y, Yang D, Wang K, Wang L, Fan J (2020) A quality diagnosis method of GMAW based on improved empirical mode decomposition and extreme learning machine. Journal of Manufacturing Processes 54:120–128. https://doi.org/10.1016/j.jmapro.2020.03.006
79. Huang GB, Zhu QY, Siew CK (2006) Extreme learning machine: theory and applications. Neurocomputing 70(1–3):489–501. https://doi.org/10.1016/j.neucom.2005.12.126
80. Zhang Z, Chen X, Chen H, Zhong J, Chen S (2014) Online welding quality monitoring based on feature extraction of arc voltage signal. The International Journal of Advanced Manufacturing Technology 70(9–12):1661–1671. https://doi.org/10.1007/s00170-013-5402-2
81. Barbe K, Pintelon R, Schoukens J (2009) Welch method revisited: nonparametric power spectrum estimation via circular overlap. IEEE Transactions on Signal Processing 58(2):553–565. https://doi.org/10.1109/TSP.2009.2031724
82. Huang Y, Xu S, Yang L, Zhao S, Shi Y et al (2019) Defect detection during laser welding using electrical signals and high-speed photography. Journal of Materials Processing Technology 271:394–403. https://doi.org/10.1016/j.jmatprotec.2019.04.022
83. Shin S, Jin C, Yu J, Rhee S (2020) Real-time detection of weld defects for automated welding process base on deep neural network. Metals 10(3):389. https://doi.org/10.3390/met10030389
84. Zhang Z, Chen S (2017) Real-time seam penetration identification in arc welding based on fusion of sound, voltage and spectrum signals. Journal of Intelligent Manufacturing 28(1):207–218. https://doi.org/10.1007/s10845-014-0971-y
85. Zhang Z, Chen H, Xu Y, Zhong J, Lv N, Chen S (2015) Multisensor-based real-time quality monitoring by means of feature extraction, selection and modeling for al alloy in arc welding.

Mechanical Systems and Signal Processing 60:151–165. https://doi.org/10.1016/j.ymssp.2014.12.021
86. Zhang Z, Wen G, Chen S (2016) Multisensory data fusion technique and its application to welding process monitoring. In: 2016 IEEE Workshop on advanced robotics and its social impacts (ARSO), IEEE, pp 294–298. https://doi.org/10.1109/ARSO.2016.7736298
87. Deng F, Huang Y, Lu S, Chen Y, Chen J, Feng H, Zhang J, Yang Y, Hu J, Lam TL et al (2020) A multi-sensor data fusion system for laser welding process monitoring. IEEE Access 8:147349–147357. https://doi.org/10.1109/ACCESS.2020.3015529
88. Griffin D, Lim J (1984) Signal estimation from modified short-time fourier transform. IEEE Transactions on Acoustics, Speech, and Signal Processing 32(2):236–243. https://doi.org/10.1109/ICASSP.1983.1172092
89. Daubechies I (1990) The wavelet transform, time-frequency localization and signal analysis. IEEE Transactions on iInformation Theory 36(5):961–1005. https://doi.org/10.1109/18.57199
90. Huang NE, Shen Z, Long SR, Wu MC, Shih HH, Zheng Q, Yen NC, Tung CC, Liu HH (1998) The empirical mode decomposition and the Hilbert spectrum for nonlinear and non-stationary time series analysis. Proceedings of the Royal Society of London Series A: Mathematical, Physical and Engineering Sciences 454(1971):903–995. https://doi.org/10.1098/rspa.1998.0193
91. Wu Z, Huang NE (2009) Ensemble empirical mode decomposition: a noise-assisted data analysis method. Advances in Adaptive Data Analysis 1(01):1–41. https://doi.org/10.1142/S1793536909000047
92. Torres ME, Colominas MA, Schlotthauer G, Flandrin P (2011) A complete ensemble empirical mode decomposition with adaptive noise. In: 2011 IEEE international conference on acoustics, speech and signal processing (ICASSP), IEEE, pp 4144–4147. https://doi.org/10.1109/ICASSP.2011.5947265
93. Portnoff M (1980) Time-frequency representation of digital signals and systems based on short-time fourier analysis. IEEE Transactions on Acoustics, Speech, and Signal Processing 28(1):55–69. https://doi.org/10.1109/TASSP.1980.1163359
94. Allen JB, Rabiner LR (1977) A unified approach to short-time fourier analysis and synthesis. Proceedings of the IEEE 65(11):1558–1564. https://doi.org/10.1109/PROC.1977.10770
95. Holschneider M, Kronland-Martinet R, Morlet J, Tchamitchian P (1990) A real-time algorithm for signal analysis with the help of the wavelet transform. In: Wavelets, Springer, pp 286–297. https://doi.org/10.1007/978-3-642-75988-8_28
96. Graps A (1995) An introduction to wavelets. IEEE Computational Science and Engineering 2(2):50–61. https://doi.org/10.1109/99.388960
97. Shensa MJ et al (1992) The discrete wavelet transform: wedding the a trous and mallat algorithms. IEEE Transactions on Signal Processing 40(10):2464–2482. https://doi.org/10.1109/78.157290
98. Gaci S (2016) A new ensemble empirical mode decomposition (EEMD) denoising method for seismic signals. Energy Procedia 97:84–91. https://doi.org/10.1016/j.egypro.2016.10.026
99. Yeh JR, Shieh JS, Huang NE (2010) Complementary ensemble empirical mode decomposition: a novel noise enhanced data analysis method. Advances in Adaptive Data Analysis 2(02):135–156. https://doi.org/10.1142/S1793536910000422
100. Jiang L, Tan H, Li X, Chen L, Yang D (2019) Ceemdan-based permutation entropy: a suitable feature for the fault identification of spiral-bevel gears. Shock and Vibration 2019. https://doi.org/10.1155/2019/7806015
101. Bissell A (1969) Cusum techniques for quality control. Journal of the Royal Statistical Society: Series C (Applied Statistics) 18(1):1–25. https://doi.org/10.2307/2346436
102. Hotelling H (1933) Analysis of a complex of statistical variables into principal components. Journal of Educational Psychology 24(6):417. https://doi.org/10.1037/h0071325
103. Quinlan JR (1986) Induction of decision trees. Machine Learning 1(1):81–106. https://doi.org/10.1007/BF00116251
104. Suykens JA, Vandewalle J (1999) Least squares support vector machine classifiers. Neural Processing Letters 9(3):293–300. https://doi.org/10.1023/A:1018628609742
105. Rish I, et al. (2001) An empirical study of the naive Bayes classifier. In: IJCAI 2001 workshop on empirical methods in artificial intelligence, vol 3, pp 41–46
106. Van Der Malsburg C (1986) Frank rosenblatt: principles of neurodynamics: perceptrons and the theory of brain mechanisms. In: Brain theory, Springer, pp 245–248, https://doi.org/10.1007/978-3-642-70911-1_20
107. McCulloch WS, Pitts W (1943) A logical calculus of the ideas immanent in nervous activity. The Bulletin of Mathematical Biophysics 5(4):115–133. https://doi.org/10.1007/BF02478259
108. LeCun Y, Bengio Y, Hinton G (2015) Deep learning. Nature 521(7553):436–444. https://doi.org/10.1038/nature14539
109. Yegnanarayana B (2009) Artificial neural networks. PHI Learning Pvt, Ltd
110. Deng L, Yu D (2014) Deep learning: methods and applications. Foundations and Trends in Signal Processing 7(3–4):197–387. https://doi.org/10.1561/2000000039
111. Razzak MI, Naz S, Zaib A (2018) Deep learning for medical image processing: overview, challenges and the future. Classification in BioApps:323–350. https://doi.org/10.1007/978-3-319-65981-7_12
112. Min S, Lee B, Yoon S (2017) Deep learning in bioinformatics. Briefings in Bioinformatics 18(5):851–869. https://doi.org/10.1093/bib/bbw068
113. LeCun Y, Bottou L, Bengio Y, Haffner P (1998) Gradient-based learning applied to document recognition. Proceedings of the IEEE 86(11):2278–2324. https://doi.org/10.1109/5.726791
114. Simonyan K, Zisserman A (2014) Very deep convolutional networks for large-scale image recognition. arXiv:14091556
115. Szegedy C, Liu W, Jia Y, Sermanet P, Reed S, Anguelov D, Erhan D, Vanhoucke V, Rabinovich A (2015) Going deeper with convolutions. In: Proceedings of the IEEE conference on computer vision and pattern recognition, pp 1–9. https://doi.org/10.1109/CVPR.2015.7298594
116. Rumelhart DE, Hinton GE, Williams RJ (1985) Learning internal representations by error propagation. California Univ San Diego La Jolla Inst for Cognitive Science, Tech. rep
117. Goodfellow IJ, Pouget-Abadie J, Mirza M, Xu B, Warde-Farley D, Ozair S, Courville A, Bengio Y (2014) Generative adversarial networks. arXiv:14062661. https://doi.org/10.1145/3422622
118. Howard AG, Zhu M, Chen B, Kalenichenko D, Wang W, Weyand T, Andreetto M, Adam H (2017) Mobilenets: efficient convolutional neural networks for mobile vision applications. arXiv:170404861
119. Zhang X, Zhou X, Lin M, Sun J (2018) Shufflenet: An extremely efficient convolutional neural network for mobile devices. In: Proceedings of the IEEE conference on computer vision and pattern recognition, pp 6848–6856. https://doi.org/10.1109/CVPR.2018.00716
120. Kiranyaz S, Ince T, Hamila R, Gabbouj M (2015) Convolutional neural networks for patient-specific ECG classification. In: 2015 37th Annual international conference of the IEEE engineering in medicine and biology society (EMBC), IEEE, pp 2608–2611. https://doi.org/10.1109/EMBC.2015.7318926